Inorganic Chemistry

Article

pubs.acs.org/IC

Copper Lanthanide Phosphonate Cages: Highly Symmetric $\{Cu_3Ln_9P_6\}$ and $\{Cu_6Ln_6P_6\}$ Clusters with C_{3v} and D_{3h} Symmetry

Eufemio Moreno Pineda,[†,‡] Christian Heesing,[§] Floriana Tuna,[†] Yan-Zhen Zheng,[†,∥] Eric J. L. McInnes,*[,†] Jürgen Schnack,[§] and Richard E. P. Winpenny*[,†]

[†]School of Chemistry and Photon Science Institute, The University of Manchester, Oxford Road, Manchester M13 9PL, U.K.

[§]Faculty of Physics, University of Bielefeld, Universitätsstrasse 25, D-33615 Bielefeld, Germany

Supporting Information

ABSTRACT: Two families of copper lanthanide phosphonate clusters have been obtained through reaction of $[Cu_2(O_2C^tBu)_4(HO_2C^tBu)_2]$ and either $Ln(NO_3)_3{\cdot}nH_2O$ or $[Ln_2(O_2C^tBu)_6(HO_2C^tBu)_6]$ and *tert*-butylphosphonic acid or an amino-functionalized phosphonic acid. The clusters, with general formula $[Cu(MeCN)_4][Cu_3Ln_9(\mu_3\text{-}OH)_7(O_3P^tBu)_6(O_2C^tBu)_{15}]$ and $[Cu_6Ln_6(\mu_3\text{-}OH)_6(O_3PC(NH_2)Me_2)_6(O_2C^tBu)_{12}]$, were structurally characterized through single crystal X-ray diffraction and possess highly symmetric metal cores with approximately C_{3v} and D_{3h} point symmetry, respectively. We have investigated the possible application of the isotropic analogues in magnetic cooling, where we were able to observe that up to around 70% of the theoretical magnetic entropy change is obtained. Simulation of the magnetic data shows antiferromagnetic coupling between the spin centers, which explains the magnetic entropy value observed.

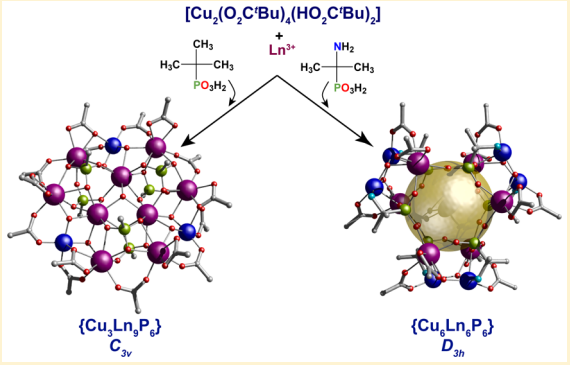

INTRODUCTION

The serendipitous assembly of polymetallic compounds can lead to interesting physical properties, even where the synthetic chemist does not possess full chemical control over the product of the reactions. An example is the $[Mn_{12}O_{12}(O_2CMe)_{16}(H_2O)_4]$ cage, that was first proposed in the early 1920s by Weinland and Fischer,[1] but which was not fully structurally characterized until 1980,[2] and where the magnetism was not understood until the 1990s.[3] This happy accident, best known as $\{Mn_{12}\}$, was the first molecule to show slow relaxation of magnetization, and hence the first single molecule magnet (SMM). Since then, many aesthetically pleasant cages, obtained from serendipitous self-assembly, have been reported, along with several proposals of futuristic applications, such as in data storage devices,[4] spintronics,[5] and quantum computing.[6] Recently, substantial work has been devoted to the implementation of molecular cages as magnetic coolants to reach the sub-kelvin regime $T < 1$ K, for which the rare and expensive ^{3}He is currently used.[7,8] Such implementation is based upon the magnetocaloric effect, which is dependent on the spin degeneracy of the system through $\sum R \ln(2S+1)$ (where R is the gas constant, and S is the spin of the ground state).[7] Ideal molecular magnetic coolants are characterized by high spin degeneracy through weak ferromagnetic exchange interactions, and low magnetic anisotropy.[9]

3d−4f mixed metal systems have been extensively studied due to the ferromagnetic interactions exhibited between them.[12] Weak interactions, high spin degeneracy, and negligible anisotropy make Gd(III) ($^8S_{7/2}$) an ideal candidate for magnetic cooling applications;[13] highly anisotropic lanthanides such as Tb(III) ($^7F_6$), Dy(III) ($^6H_{15/2}$), Ho(III) ($^5I_8$), and Er(III) ($^4I_{15/2}$), which impose slow relaxation characteristics, are the preferred lanthanides for single molecule magnets;[14] the high anisotropy makes them unsuitable as components of magnetic coolants.

To achieve high nuclearity cages, numerous ligands have been employed.[10,11] Phosphonates[15,16] have become increasingly popular due to the convenience of tuning the R groups and the diversity of binding modes observed. Introduction of preformed metal cages and coligands in the synthesis have proven successful in producing discrete species.[16] We have recently reported the synthesis of several 3d−4f clusters with considerable high magnetic entropy ($-\Delta S_m$) such as $\{Ni_6Gd_6P_6\}$,[15a] $\{Fe_6Gd_6P_6\}$,[15b] $\{Cr_6Gd_2P_2\}$,[15c] $\{Mn_9Gd_9P_{12}\}$,[15d] $\{Mn_4Gd_6P_6\}$,[15d] and $\{Co_xGd_yP_z\}$,[15e,f] where phosphonates prove successful in coordinating several metal centers into a single molecule. Furthermore, the introduction of further functionalities to the R group of the phosphonates led to two molecules, namely, $\{Co_4Ln_{10}P_{10}\}$ and $\{Co_6Ln_4P_6\}$, showing that functionalization of phosphonate ligands is a very promising route to obtain further 3d−4f cages.[15g] Lately this method has also afforded discrete species composed of homometallic lanthanide phosphonates.[16]

Received: March 24, 2015
Published: June 10, 2015

DOI: 10.1021/acs.inorgchem.5b00649
Inorg. Chem. 2015, 54, 6331−6337

Here we report further 3d−4f phosphonate cages. In one family the copper precursor was $[Cu_2(O_2C^tBu)_4(HO_2C^tBu)_2]$ reacted with $Ln(NO_3)_3{\cdot}nH_2O$ and *tert*-butylphosphonic acid producing a highly symmetrical family of $\{Cu_3Ln_9P_6\}$ cages with general formula $[Cu_3Ln_9(\mu_3\text{-}OH)_7(O_3P^tBu)_6(O_2C^tBu)_{15}][Cu(MeCN)_4]$ where Ln = Gd(III), **1**; Tb(III), **2**; Dy(III), **3**; Ho(III), **4**; and Er(III), **5**. Functionalization of the R group with an amino functionality yielded a second family of cages with general formula $[Cu_6Ln_6(\mu_3\text{-}OH)_6(O_3PC(NH_2)Me_2)_6(O_2C^tBu)_{12}]$ (where Ln = Gd(III), **6**; Tb(III), **7**; Dy(III), **8**; and Ho(III), **9**) possessing D_{3h} symmetry. Here we report the magnetic behavior of these systems and explore the possibility of the application of such compounds in magnetic cooling. We have modeled the magnetic behavior of the Gd(III)-containing systems despite the gigantic Hilbert space involved. Quasi-exact methods allow the determination of the exchange interaction for $\{Cu_3Gd_9P_6\}$, while for the $\{Cu_6Gd_6P_6\}$ analogue, we have taken advantage of the symmetry to model the magnetic data.

EXPERIMENTAL SECTION

Starting Materials. $[Cu_2(O_2C^tBu)_4(HO_2C^tBu)_2]$[17] and $[Ln_2(O_2C^tBu)_6(HO_2C^tBu)_6]$[18] (Ln = Gd(III), Tb(III), Dy(III), Ho(III), and Er(III)) were prepared by literature methods. Solvents and starting materials were used as purchased. Elemental analyses were performed by the microanalytical service of The University of Manchester (Table S1 in the Supporting Information).

Synthesis of $\{Cu_3Ln_9P_6\}$. Compounds **1** to **5** were obtained by mixing $[Cu_2(O_2C^tBu)_4(HO_2C^tBu)_2]$ (18 mg, 0.024 mmol) and $Ln(NO_3)_3{\cdot}nH_2O$ (0.1 mmol) (Ln = Gd(III), Tb(III), Dy(III), Ho(III), or Er(III)) in MeCN (16 mL) for 15 min. After this period a solution of $H_2O_3P^tBu$ (14 mg, 0.1 mmol) and Et_3N (0.1 mL, 1 mmol) in MeCN (4 mL) was added. The resulting solution was refluxed for 3 h, and then filtered. Blue hexagonal-shaped X-ray quality crystals of $[Cu_3Ln_9(\mu_3\text{-}OH)_7(O_3P^tBu)_6(O_2C^tBu)_{15}][Cu(MeCN)_4]$ (Ln = Gd(III), **1**; Tb(III), **2**; Dy(III), **3**; Ho(III), **4**; or Er(III), **5**) were collected after 2 weeks of slow evaporation crystallization.

Synthesis of (1-Amino-1-methylethyl)phosphonic Acid.[19] A solution of acetone (6.3 mL, 0.085 mol), diethyl phosphite (11 mL, 0.085 mol), and NH_3/EtOH (50 mL, 0.1 mol) was heated in a sealed ampule to 100 °C for 3 h, followed by removal of the excess NH_3 and EtOH under reduced pressure. The resulting oily solution was a mixture of diethyl (1-amino-1-methylethyl)phosphonate and diethyl phosphite. The oily product (13 g) was then dissolved in acetone (38 mL), and a solution of oxalic acid (5.4 g, 0.06 mol) in acetone (13.7 mL) was added. The mixture was refrigerated overnight, and the precipitated product was separated by filtration and washed with cold acetone (3 × 25 mL). The dry product was treated with a saturated solution of $NaHCO_3$ and then extracted with dichloromethane (DCM) until the extracted DCM became colorless (see Scheme 1). Then the solution was concentrated in vacuo to give pure diethyl (1-amino-1-methylethyl)phosphonate (8 g, 48.2%).

Synthesis of $\{Cu_6Ln_6P_6\}$. A solution of $[Cu_2(O_2C^tBu)_4(HO_2C^tBu)_2]$ (0.165 g, 0.22 mmol) and $[Ln_2(O_2C^tBu)_6(HO_2C^tBu)_6]$ (Ln = Gd(III), Tb(III), Dy(III), and Ho(III)) (0.3 mmol) in MeCN (18 mL) was prepared and stirred for 15 min. (1-Amino-1-methylethyl)phosphonic acid (0.082 g, 0.6 mmol) and $^iPrNH_2$ (0.2 mL, 2.4 mmol) in H_2O (2 mL) was added, and the resulting solution was refluxed for 3 h. It was then allowed to cool to room temperature and filtered. Blue block-shaped X-ray quality crystals of $[Cu_6Ln_6(\mu_3\text{-}OH)_6(O_3PC(NH_2)Me_2)_6(O_2C^tBu)_{12}]$ (Ln = Gd(III), **6**; Tb(III), **7**; Dy(III), **8**; and Ho(III), **9**) were obtained after 2 weeks of slow evaporation.

Scheme 1. Schematic Description of Synthesis of 1-Amino-1-methyl-ethylphosphonic Acid

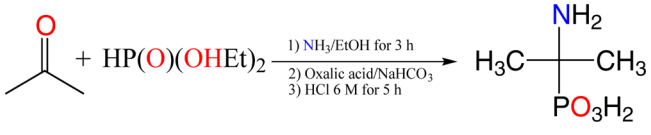

X-ray Data Collection and Structure Solution. The data of **1**, **4**, **5**, **7**, and **8** were collected on an Agilent SUPERNOVA diffractometer with Mo Kα radiation (λ = 0.71073 Å). Single crystal X-ray diffraction measurement for **3** and **6** were carried out on a Bruker SMART CCD diffractometer with Mo Kα radiation (λ = 0.71073 Å) at 100 K. Data for **3** was collected on a Rigaku Saturn724+ diffractometer (synchrotron, λ = 0.68890 Å) at beamline I19 at DIAMOND Light Source, U.K. Data reduction and unit cell refinement for all systems were performed with Crysallis software. The structures were solved by direct methods using SHELXS[20a] and were refined by full-matrix least-squares methods using Olex2.[20b] In all cases the crystals were mounted on a tip using crystallographic oil and placed in a cryostream. Data were collected using ϕ and ω scans chosen to give a complete asymmetric unit. All non-hydrogen atoms were refined anisotropically, while hydrogen atoms were calculated geometrically riding on their respective atoms.

Large solvent accessible voids were found for complexes **6** to **9**. However, the location of discrete solvent molecules could not be determined by simple refinement, therefore the contents of the large voids on the crystal structure were determined using the solvent-masking procedure SQUEEZE using Platon.[20c]

Crystal data and refinement parameters are given in Table S2 in the Supporting Information and have been deposited with CCDC codes 1053725−1053732. These data can be obtained free of charge via www.ccdc.cam.ac.uk/conts/retrieving.html (or from the Cambridge Crystallographic Data Centre, 12 Union Road, Cambridge CB21EZ, U.K.; fax (+44)1223-336-033; or deposit@ccdc.cam.ac.uk).

Magnetic Measurements. The magnetic behavior of complexes **1** to **9** was studied with a Quantum Design MPMS-XL7 SQUID magnetometer employing ground samples placed in a gel capsule and fixed with a small amount of eicosane to avoid movement during the measurement. The diamagnetic contribution from the gel capsule and the eicosane were corrected using experimental data obtained for such diamagnetic matrices and the diamagnetic contribution from the complexes calculated from Pascal constants.[21]

RESULTS AND DISCUSSION

Synthetic Description. Reflux reactions of $[Cu_2(O_2C^tBu)_4(HO_2C^tBu)_2]$, $Ln(NO_3)_3{\cdot}nH_2O$, and *tert*-butylphosphonic acid led to $\{Cu_3Ln_9P_6\}$ in reasonable yield (17−31%), obtained through slow evaporation crystallization. Single crystal X-ray diffraction identified the products as $[Cu(MeCN)_4][Cu_3Ln_9(\mu_3\text{-}OH)_7(O_3P^tBu)_6(O_2C^tBu)_{15}]$. The presence of $[Cu(MeCN)_4]^+$ could be explained as the reduction product of the $[Cu_2(O_2C^tBu)_4(HO_2C^tBu)_2]$ in the presence of free carboxylic acid, as previously seen.[22] Similarly a family of highly symmetrical $\{Cu_6Ln_6P_6\}$ were obtained after refluxing $[Cu_2(O_2C^tBu)_4(HO_2C^tBu)_2]$, $[Ln_2(O_2C^tBu)_6(HO_2C^tBu)_6]$, and an amino-functionalized phosphonate source, (1-amino-1-methylethyl)phosphonic acid. Single crystal X-ray analysis revealed the products to be $[Cu_6Ln_6(\mu_3\text{-}OH)_6(O_3PC(NH_2)Me_2)_6(O_2C^tBu)_{12}]$ in (20−36%) yield.

In our approach we have used two phosphonate sources, which led to high nuclearity discrete compounds. First, reaction of *tert*-butylphosphonic acid along with a preformed copper carboxylate dimer and a simple lanthanide salt gives oligonuclear $\{Cu_3Ln_9P_6\}$ species. In our second approach we employed a functionalized phosphonate, (1-amino-1-methylethyl)phosphonic acid, that due to its higher polarity presented compared to $^tBuPO_3H_2$ required the addition of a small amount of water to the reaction. We first react (1-amino-1-methylethyl)phosphonic acid with $[Cu_2(O_2C^tBu)_4(HO_2C^tBu)_2]$, $Ln(NO_3)_3{\cdot}nH_2O$, and Et_3N.

DOI: 10.1021/acs.inorgchem.5b00649
Inorg. Chem. 2015, 54, 6331−6337

Under these conditions a gel-like material was formed, which we were unable to characterize, probably due to the formation of a polymeric material due to the extra binding mode of the amino group present in the phosphonate source; we therefore used a preformed lanthanide carboxylate dimer as a substrate to prevent the formation of the insoluble polymeric material and replace the EtN_3 by $^{i}PrNH_2$ to optimize the reaction. This leads to $\{Cu_6Ln_6P_6\}$ species, where the metal sites are again arranged in a highly symmetrical array. It is important to stress that while the presence of a mild base such Et_3N in the reaction of $\{Cu_3Ln_9P_6\}$ is to deprotonate the phosphonate source, in the case of the synthesis of $\{Cu_6Ln_6P_6\}$, the $^{i}PrNH_2$ may also template the molecule through hydrogen bonding with the oxygens of the phosphonate groups.

Structural Description. *{$Cu_3Ln_9P_6$}.* Single crystal X-ray diffraction of **1** to **5** shows these to be $[Cu_3Ln_9(\mu_3\text{-}OH)_7(O_3P^tBu)_6(O_2C^tBu)_{15}][Cu(MeCN)_4]$ (Ln = Gd(III), **1**; Tb(III), **2**; Dy(III), **3**; Ho(III), **4**; and Er(III), **5**) (Figure 1). The

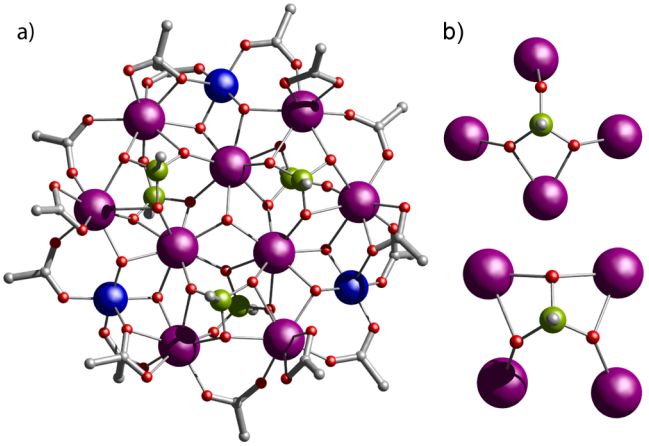

Figure 1. (a) Crystal structure of $[Cu_3Dy_9(\mu_3\text{-}OH)_7(O_3P^tBu)_6(O_2C^tBu)_{15}]^-$ viewed along the C_3 axis; (b) coordination modes of phosphonates. Color code: Dy, purple; Cu, blue; P, green; O, red; C, gray. ^{t}Bu groups on carboxylates and phosphonates and hydrogens were removed for clarity.

clusters crystallize as anions with $[Cu(MeCN)_4]^+$ cations (Figure S1 in the Supporting Information), in the space group $R3$ with $Z = 3$, and have an overall C_{3v} symmetry. The crystallographic description of the anion of **3** is given as representative. Three Dy(III) atoms with Ln···Ln distances of 3.884(1) Å form a triangle inside a $\{Cu_3Dy_6\}$ ring (Figure 1). In the nonagon, a Cu(II) is found between each two Dy(III) ions with Cu···Dy distances ranging between 3.455(3) and 3.767(3) Å, and Dy···Dy of 4.276(2) Å. The nine Dy(III) sites have dodecahedral coordination geometries, and three Cu(II) sites have five-coordinate square pyramidal geometries (Figure 1).

The metal ions in the anionic cage are bridged by a total of 15 pivalates, six fully deprotonated phosphonates, and seven hydroxides. The metal ions are sandwiched between two phosphonate triangles. One of the triangles is composed of phosphonates with a bridging mode 4.222 while the other has a 4.221 mode (Harris notation).[23] Pivalate groups adopt 1.11, 2.11, or 2.21 coordination modes, the 2.21 pivalate chelating to a Dy(III) site and bridging to a copper. Each copper is also bridged by two hydroxides to two adjacent Dy(III) and one Dy(III) of the inner triangle with distances of 1.945(9) and 1.99(1) Å (Cu···O). Finally, each Dy(III) atom in the inner triangle is bridge by one μ_3-OH at a Dy···O distance of 2.387(1) Å.

{$Cu_6Ln_6P_6$}. Structural X-ray analysis of compounds **6** to **9** reveals a family of cages of formula $[Cu_6Ln_6(\mu_3\text{-}OH)_6(O_3PC(NH_2)Me_2)_6(O_2C^tBu)_{12}]$ (Ln = Gd(III), **6**; Tb(III), **7**; Dy(III), **8**; and Ho(III), **9**) (Figure 2 and Figure S2 in the Supporting Information). All clusters crystallize in the space group *Fddd* with $Z = 16$ and an overall D_{3h} symmetry with one half of the molecule in the asymmetric unit. The structure of **1** is described as representative.

The $\{Gd_6P_6\}$ core (Figure 2) resembles the double-six-ring (D6R or 6−6) building block unit found in zeolites.[24] The interaction between the oxygen atoms of the phosphonate and the hydrogens of the $^{i}PrNH_2$ template the metal core, featuring a cylindrical drum with a hexagonal prism form, whose top and bottom faces are made up of 12-membered $\{Gd_3O_6P_3\}$ rings (including the oxygen atoms). The top and bottom faces are linked by six oxygens interconnecting one Gd(III) and one phosphonate (Gd−O−P), to give an alternated $\{Gd_6O_{18}P_6\}$ hexagonal prism. All aminophosphonates exhibit a 4.2111 coordination mode. In each case the amino group is terminally bound to Cu(II), while one O-donor bridges between a Cu(II) and a Gd(III). Two μ_3-OH connect two Cu(II) ions and a Gd(III) ion with the top and bottom face of the cluster. If just the Cu(II), Gd(III), μ_3-OH, and P are considered, this fragment resembles a distorted cubane. Three other 2.11 pivalates interconnect one Gd(III) ion with a Cu(II). **6** is formed by three distorted cubane fragments, with two crystallographically different $\{Cu_2Gd_2P_2\}$ moieties (see Table S3 in the Supporting Information). For example, in **6** two Cu···Cu distances (2.958(1) and 2.986(1) Å) and three Cu···O···Cu angles (96.2(2), 97.3(2), and 98.3(2)°) are observed. All Gd(III) ions exhibit O-bound capped octahedral geometry with one 1.11 pivalate capping the octahedron, while all Cu(II) ions exhibit a square pyramidal geometry.

Magnetic Description. Magnetic susceptibility studies on **1**−**9** were performed on polycrystalline samples in the temperature range 2−300 K under an applied dc magnetic field (H) of 0.1 kOe. Magnetization as a function of applied field was investigated in the field and temperature ranges 0−7 T and 2−10 K, respectively.

For compounds **1**−**9** room temperatures $\chi_M T$ values (where χ_M is molar susceptibility) are close to those expected for non-interacting ions (results are summarized in Table 1 along with relevant parameters (S, L, J, g_J)). For all four complexes there is a minimum in $\chi_M T$ at a few Kelvins; this may be a signature of weak intramolecular magnetic interactions.

A gradual decrease of the $\chi_M T$ with decreasing temperature is observed for all nonisotropic lanthanide containing cages, due to the depopulation of the Stark levels and/or possible presence of antiferromagnetic interactions (Figures S5 and S6 in the Supporting Information). Field dependent magnetization measurements were performed at between 1.8 and 5 K, and the values obtained for complexes **1**−**9** at 2 K and 7 T are summarized in Table 1.

Understanding the magnetic behavior of polymetallic compounds containing Tb(III), Dy(III), Ho(III), and Er(III) is difficult due to their anisotropic character as depopulation of the Stark levels has a similar effect on the variable temperature magnetic properties as antiferromagnetic exchange interactions. Modeling the magnetic behavior of complexes containing the isotropic Gd(III) is far easier, although still challenging due to the very large size of the problem. For compound **1**, the room

DOI: 10.1021/acs.inorgchem.5b00649
Inorg. Chem. 2015, 54, 6331−6337

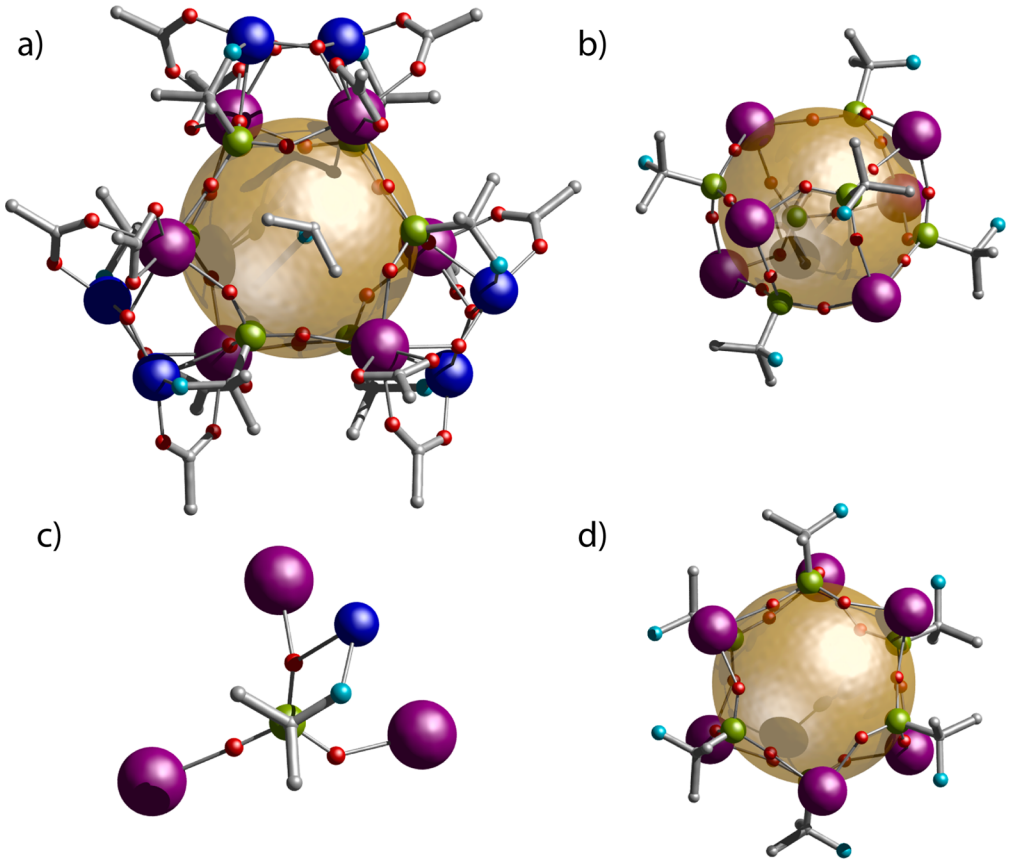

Figure 2. (a) Crystal structure of $[Cu_6Gd_6(\mu_3\text{-}OH)_6(O_3PC(NH_2)Me_2)_6(O_2C^tBu)_{12}]$ viewed along the C_3 axis; (b, d) 4f-phosphonate metal core with D6R-like core; (c) phosphonate coordination mode in the cage. Color code: Gd, purple; Cu, blue; P, green; O, red; N, light blue; C, gray. ^{t}Bu groups on carboxylates and hydrogens were removed for clarity.

Table 1. Magnetic Data for 1−5

	1	2[d]	3[d]	4[d]	5	6	7	8	9
S (Cu^{2+})	1/2	1/2	1/2	1/2	1/2	1/2	1/2	1/2	1/2
S (Ln^{3+})	7/2	3	5/2	2	3/2	7/2	3	5/2	2
L (Ln^{3+})	0	3	5	6	6	0	3	5	6
J (Ln^{3+})	7/2	6	15/2	8	15/2	7/2	6	15/2	8
g_J (Ln^{3+})	2	3/2	4/3	5/4	6/5	2	3/2	4/3	5/4
g (Cu^{2+})	2	2	2	2	2	2	2	2	2
$\chi_M T$ (calcd)[b]	72.0	107.4	128.6	127.7	104.4	49.5	73.1	87.2	86.6
$\chi_M T$ (obs)[b]	72.1	106.2	128.3	124.4	104.9	48.7	71.7	86.4	85.1
$\chi_M T$ (at 2 K)[b]	34.6	32.2	64.7	40.1	54.1	41.2	33.5	57.5	42.2
M (obs)[c]	64.0	45.2	49.1	48.7	52.2	41.3	28.5	32.8	35.9

[a] S (total spin angular momentum), L (total orbital angular momentum), and J (total angular momentum), of the ground multiplet. g_J is the Landé factor. [b] Values of $\chi_M T$ are given in emu mol^{-1} K. [c] Values of M are given in μ_B. [d] Magnetization measured at 1.8 K.

temperature value is close to that expected for the non-interacting ions (Table 1). Upon cooling the $\chi_M T$ stays practically constant up to about 40 K, where it sharply decreases. The $M(H)$ was also investigated at different applied fields and temperatures revealing no saturation at the highest field and lowest temperature, i.e., 7 T and 2 K. This observation is consistent with the behavior observed in the $\chi_M T$ at low temperatures. The magnetic data $\chi_M T(T)$ and $M(H)$ could be fitted despite the challenging dimension of the Hilbert space ($(2S_i + 1)^n \times (2S_j + 1)^m = 1073741824$, where $n = 9$ and $m = 3$). Modern quasi-exact approximations, such as finite-temperature Lanczos method, which is a Krylov-space method, has proven to be very accurate to solve such problems.[25]

Many exchange paths are in principle possible. The C_{3v} symmetry suggests at least four exchange interactions J_1, J_2, J_3, J_4. However, it turned out that a parameter set where nearest neighbor interaction pathways are equivalent ($J_1 = J_3$, $J_2 = J_4$, see inset in Figure 3a) is sufficient to model the data. Then the Hamiltonian reads

$$\hat{H} = -2J_1 \sum_{i,j=n.n.} \hat{S}_{Gd_i} \cdot \hat{S}_{Gd_j} - 2J_2 \sum_{i,j=n.n.} \hat{S}_{Cu_i} \cdot \hat{S}_{Gd_j} + \mu_B B_z (g_{Gd} \sum_i \hat{S}_{z_{Gd_i}} + g_{Cu} \sum_j \hat{S}_{z_{Cu_j}}) \quad (1)$$

DOI: 10.1021/acs.inorgchem.5b00649
Inorg. Chem. 2015, 54, 6331−6337

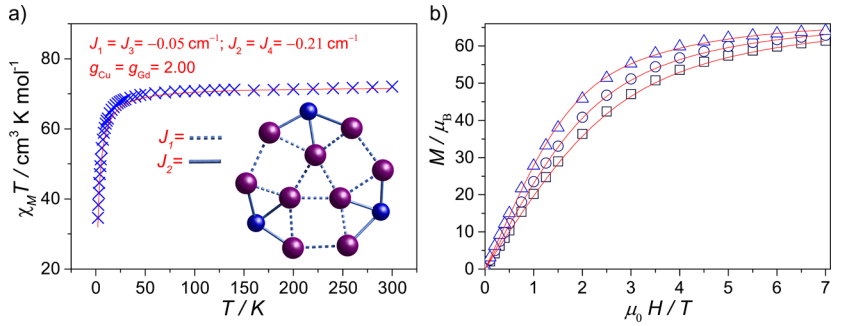

Figure 3. (a) Molar magnetic susceptibility $\chi_M T$ vs T plot and simulation for **1** under 1 kG dc field. (b) Molar magnetization $M(H)$ and simulation for **1**. Red traces are simulation with parameter in the text.

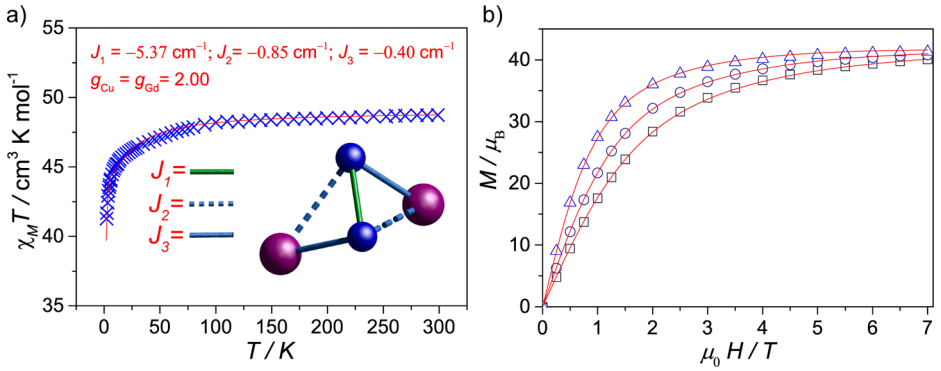

Figure 4. (a) Molar magnetic susceptibility $\chi_M T$ vs T plot and simulation for **6** under 1 kG dc field, (b) Molar magnetization $M(H)$ and simulation for **6**. Red traces are simulation with parameter in the text.

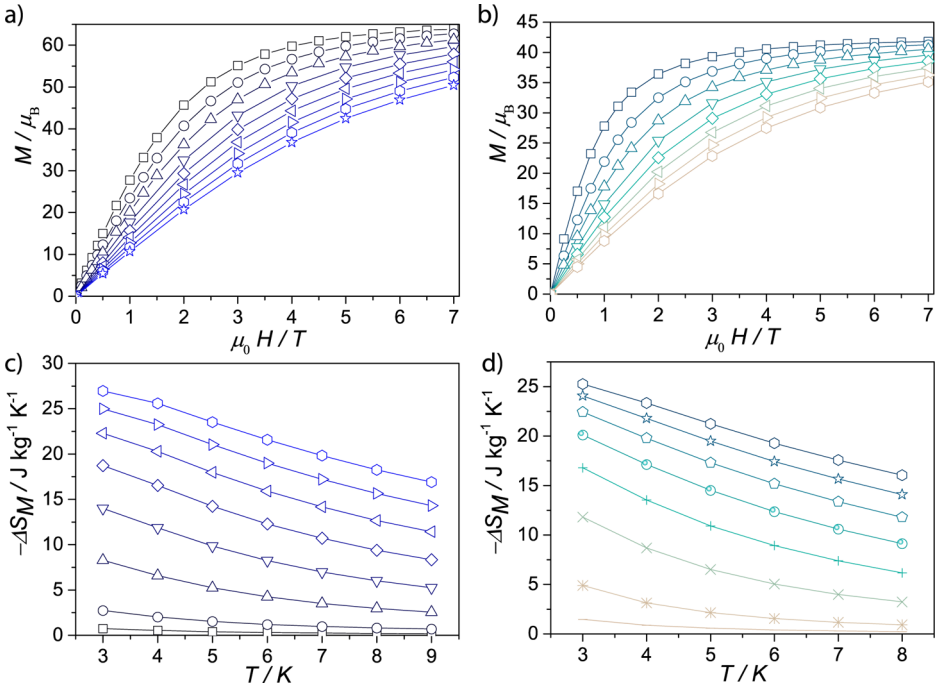

Figure 5. M/μ_B vs H at different temperatures (a) for compound **1** and (b) for compound **6**. Magnetic entropy change (c) for compound **1** and (d) for compound **6**.

Here the first term accounts for the exchange interaction between the nearest Gd(III) neighbors, the second term takes into account the interactions between the Cu(II) ions and their nearest Gd(III) neighbors, and the third term is the Zeeman interaction. Agreement between experiment and simulations is achieved with two exchange interactions; $J_1 = J_3 = -0.05$ cm^{-1} and $J_2 = J_4 = -0.21$ cm^{-1} (Figure 3) assuming an isotropic g-factor for Cu(II) and Gd(III) of $g = 2.0$.

The magnetic data of **6** have been modeled using a different approach. Due to the symmetry of the system, D_{3h} (crystallo-

DOI: 10.1021/acs.inorgchem.5b00649
Inorg. Chem. 2015, 54, 6331−6337

graphically half of the molecule is present in the asymmetric unit, with two very similar $\{Cu_2Gd_2\}$ fragments), and the long distances observed between Gd(1)···Gd(1)′ and Gd(2)···Gd(2)′ we have simulated the data of a third of the fragment assuming three independent $\{Cu_2Gd_2\}$ moieties. Simultaneous fitting[26] of $\chi_M T(T)$ and $M(H)$ allowed determination of the parameters of the following Hamiltonian (eq 2) with $S_{Cu} = 1/2$, $g_{Cu} = 2.0$, $S_{Gd} = 7/2$, and $g_{Gd} = 2.0$:

$$\hat{H} = -2J_1(\hat{S}_{Cu1}\cdot\hat{S}_{Cu2}) - 2J_2(\hat{S}_{Cu1}\cdot\hat{S}_{Gd2} + \hat{S}_{Cu2}\cdot\hat{S}_{Gd1}) - 2J_3(\hat{S}_{Cu1}\cdot\hat{S}_{Gd1} + \hat{S}_{Cu2}\cdot\hat{S}_{Gd2}) + g\mu_B B\sum_{i=1}^{4} S_i \quad (2)$$

In the Hamiltonian (eq 2) the first term is the isotropic exchange interaction between Cu(1)···Cu(2) bridged by two μ_3-OH with an average distance of 2.977(1) Å, while the second term represents the interaction between Cu(1)···Gd(2) and Cu(2)···Gd(1) bridged by one pivalate, a μ_3-OH, and the amino group of the phosphonate at an average distance of 3.402(1) Å, and the third term provides the interaction between Cu(1)···Gd(1) and Cu(2)···Gd(2) bridged by μ_3-OH and the amino group of the phosphonate at an average distance of 3.974(1) Å (see inset of Figure 4a). The fourth term represents the Zeeman interaction with the applied magnetic field. A good agreement was found between the experimental data and the simulation using the following parameters: $J_1 = -5.37$ cm^{-1}, $J_2 = -0.85$ cm^{-1}, and $J_3 = -0.40$ cm^{-1} (Figure 4). A relatively weak J_1 was found, a value that can be rationalized by a combination of the long Cu···O distances and small Cu···O···Cu angles, and similar values have been reported.[27] Hatfield and Hodgson have related the Cu···O···Cu angles to the nature of the exchange interaction, i.e., ferromagnetic (for angle <97.5°) or antiferromagnetic (for angle >97.5°);[28] in **6** we see angles very close to this value (see Table S3 in the Supporting Information), and hence a very small exchange interaction would be expected.

Ac susceptibility tests were performed for all anisotropic lanthanide-containing compounds. However, no out-of-field component, a typical feature of SMMs, was observed for the clusters above 2 K.

The high nuclearity, the isotropic nature of Cu(II) and Gd(III), and the relatively small exchange interaction led us to examine compounds **1** and **6** for possible magnetocaloric applications. The magnetic entropy changes of **1** and **6** were obtained from isothermal magnetization measurements from 0 to 7 T in the temperature range 2−10 K (Figure 5).

The maximum values observed for the complexes **1** and **6** at 3 K and 7 T are $-\Delta S_m = 26.9$ and 27.4 J kg^{-1} K^{-1} respectively. The magnetic entropy for non-interacting centers is given by $\sum nR\ln(2s+1)$ (R being the gas constant), leading to values of 20.8R (40.4 J kg^{-1} K^{-1}, for nine Gd(III) and three Cu(II)) for **1** and 16.6R (38.7 J kg^{-1} K^{-1}, for six Gd(III) and six Cu(II)) for **6**. Comparison of the experimental $-\Delta S_m$ with the theoretical value clearly shows that 66 and 71% (at 3 K and 7 T) of the total magnetic entropy is accessed. This fact is most likely attributable to the antiferromagnetic exchange operating within the molecules.

CONCLUSIONS

The synthesis and characterization of mixed-metal 3d−4f cages have been achieved through the synthesis of preformed carboxylate cages with phosphonates under reflux conditions, phosphonates proving successful ligands to bring several paramagnetic ions in a single entity. Similarly the functionalization of a phosphonate with an extra coordinating group leads to a family of cages, both families possessing highly symmetric motifs, the first family being described as a nonagon, with C_{3v} symmetry, while the second possesses a D6R-like metal core with D_{3h} point group symmetry. We have studied the magnetic properties of both families and the application of the isotropic cages into applications such as magnetocaloric. Simulation of the isotropic systems reveals antiferromagnetic interactions operating within each system, leading to a diminished magnetic entropy change compared to that of the non-interacting ions. The antiferromagnetic exchange interactions mean that these compounds are not of interest for magnetic cooling.

ASSOCIATED CONTENT

Supporting Information

Elemental analysis tables, crystallographic tables, figures of the packing of clusters, and figure of magnetic data and simulations for all compounds. The Supporting Information is available free of charge on the ACS Publications website at DOI: 10.1021/acs.inorgchem.5b00649.

AUTHOR INFORMATION

Corresponding Authors

*E-mail: eric.mcinnes@manchester.ac.uk.
*E-mail: Richard.Winpenny@manchester.ac.uk.

Present Addresses

‡E.M.P.: Institute of Nanotechnology, Karlsruhe Institute of Technology, D-76344, Eggenstein-Leopoldshafen, Germany.
‖Y.-Z.Z: Center for Applied Chemical Research, Frontier Institute of Science and Technology, Xi'an Jiaotong University, Xi'an 710054, China.

Notes

The authors declare no competing financial interest.

ACKNOWLEDGMENTS

E.M.P. thanks the Panamanian agency SENACYT-IFARHU. J.S. thanks the Deutsche Forschungsgemeinschaft (SCHN/615-15) for continuous support. Supercomputing time at the LRZ Garching is gratefully acknowledged. R.E.P.W. thanks the Royal Society for a Wolfson Merit Award. We also thank Dr. David Allan and his team for help in use of X-ray at the synchrotron at Diamond Light Source, and we thank DLS for beam-time.

REFERENCES

(1) Weinland, R. F.; Fischer, G. *Z. Anorg. Allg. Chem.* **1921**, *120*, 161−180.
(2) Lis, T. *Acta Crystallogr., B* **1980**, *36*, 2042−2046.
(3) (a) Caneschi, D.; Gatteschi, D.; Sessoli, R. *J. Am. Chem. Soc.* **1991**, *113*, 5874−5876. (b) Sessoli, R.; Tsai, H. L.; Schake, A. R.; Wang, S.; Vincent, J. B.; Folting, K.; Gatteschi, D.; Christou, G.; Hendrickson, D. N. *J. Am. Chem. Soc.* **1993**, *115*, 1804−1816. (c) Sessoli, R.; Gatteschi, D.; Caneschi, A.; Novak, M. A. *Nature* **1993**, *365*, 141−142.
(4) (a) Gatteschi, D.; Sessoli, R.; Villain, J. *Molecular Nanomagnets*; Oxford University Press: Oxford, U.K., 2006; pp 306−317. (b) Mannini, M.; Pineider, F.; Sainctavit, P.; Danieli, C.; Otero, E.; Sciancalepore, C.; Talarico, A. M.; Arrio, M.-A.; Cornia, A.; Gatteschi, D.; Sessoli, R. *Nat. Mater.* **2009**, *8*, 194−197.
(5) (a) Sanvito, S. *Chem. Soc. Rev.* **2011**, *40*, 3336−3355. (b) Bogani, L.; Wolfgang, W. *Nat. Mater.* **2008**, *7*, 179−186.
(6) (a) Leuenberger, M. N.; Loss, D. *Nature* **2001**, *410*, 789−793. (b) Troiani, F.; Affronte, M. *Chem. Soc. Rev.* **2011**, *40*, 3119−3129.

DOI: 10.1021/acs.inorgchem.5b00649
Inorg. Chem. 2015, 54, 6331−6337

(7) (a) Giauque, W. F.; MacDougall, D. P. *Phys. Rev.* **1933**, *43*, 768−783. (b) Sharples, J. W.; Collison, D.; McInnes, E. J. L.; Schnack, J.; Palacios, E.; Evangelisti, M. *Nat. Commun.* **2014**, *5*, 5321−5326.
(8) Evangelisti, M.; Candini, A.; Ghirri, A.; Affronte, M.; Brechin, E. K.; McInnes, E. J. L. *Appl. Phys. Lett.* **2005**, *87*, 072504.
(9) (a) Evangelisti, M.; Brechin, E. K. *Dalton Trans.* **2010**, *39*, 4672−4676. (b) Garlatti, E.; Carretta, S.; Schnack, J.; Amoretti, G.; Santini, P. *Appl. Phys. Lett.* **2013**, *103*, 202140. (c) Evangelisti, M.; Lorusso, G.; Palacios, E. *Appl. Phys. Lett.* **2014**, *105*, 046101/1. (d) Garlatti, E.; Carretta, S.; Schnack, J.; Amoretti, G.; Santini, P. *Appl. Phys. Lett.* **2014**, *105*, 046101.
(10) Accorsi, S.; Barra, A.; Caneschi, A.; Chastanet, G.; Cornia, A.; Fabretti, A. C.; Gatteschi, D.; Mortalo, C.; Olivieri, E.; Parenti, F.; Rosa, P.; Sessoli, R.; Sorace, L.; Wernsdorfer, W.; Zobbi, L. *J. Am. Chem. Soc.* **2006**, *126*, 4742−4755.
(11) (a) Brechin, E. K. *Chem. Commun.* **2005**, *41*, 5141−5153. (b) Glaser, T. *Chem. Commun.* **2011**, *47*, 116−130. (c) Cowan, M. G.; Brooker, S. *Coord. Chem. Rev.* **2012**, *256*, 2944−2971. (d) Escuer, A.; Aromí, G. *Eur. J. Inorg. Chem.* **2006**, *23*, 4721−4736.
(12) See: Winpenny, R. E. P. *Chem. Soc. Rev.* **1998**, *27*, 447−452 and references therein.
(13) Hooper, T. N.; Schnack, J.; Piligkos, S.; Evangelisti, M.; Brechin, E. K. *Angew. Chem., Int. Ed.* **2012**, *51*, 4633−4636.
(14) (a) Sorace, L.; Benelli, C.; Gatteschi, D. *Chem. Soc. Rev.* **2011**, *40*, 3092−3104. (b) Woodruff, D. N.; Winpenny, R. E. P.; Layfield, R. A. *Chem. Rev.* **2013**, *113*, 5110−5148.
(15) (a) Moreno-Pineda, E.; Tuna, F.; Zheng, Y.-Z.; Winpenny, R. E. P.; McInnes, E. J. L. *Inorg. Chem.* **2013**, *52*, 13702−13707. (b) Moreno-Pineda, E.; Tuna, F.; Zheng, Y.-Z.; Teat, S. J.; Winpenny, R. E. P.; Schnack, J.; McInnes, E. J. L. *Inorg. Chem.* **2014**, *53*, 3032−3038. (c) Zangana, K. H.; Moreno-Pineda, E.; Vitorica-Yrezabal, I. J.; McInnes, E. J. L.; Winpenny, R. E. P. *Dalton Trans.* **2014**, *43*, 13242−13249. (d) Zheng, Y.-Z.; Moreno-Pineda, E.; Helliwell, M.; Winpenny, R. E. P. *Chem.—Eur. J.* **2012**, *18*, 4161−4165. (e) Zheng, Y.-Z.; Evangelisti, M.; Winpenny, R. E. P. *Chem. Sci.* **2011**, *2*, 99−102. (f) Zheng, Y.-Z.; Evangelisti, M.; Tuna, F.; Winpenny, R. E. P. *J. Am. Chem. Soc.* **2012**, *134*, 1057−1065. (g) Moreno-Pineda, E.; Tuna, F.; Pritchard, R. G.; Zheng, Y.-Z.; Regan, A. C.; Winpenny, R. E. P.; McInnes, E. J. L. *Chem. Commun.* **2013**, *49*, 3522−3524. (h) Zheng, Y.-Z.; Breeze, B. A.; Timco, G. A.; Tuna, F.; Winpenny, R. E. P. *Dalton Trans.* **2010**, *39*, 6175−6177. (i) Zheng, Y.-Z.; Evangelisti, M.; Winpenny, R. E. P. *Angew. Chem., Int. Ed.* **2011**, *50*, 3692−3695. (j) Zheng, Y.-Z.; Winpenny, R. E. P. *Sci. China: Chem.* **2012**, *55* (6), 910−913.
(16) (a) Zangana, K. H.; Moreno-Pineda, E.; Schnack, J.; Winpenny, R. E. P. *Dalton Trans.* **2013**, *42*, 14045−14048. (b) Zangana, K. H.; Moreno-Pineda, E.; McInnes, E. J. L.; Schnack, J.; Winpenny, R. E. P. *Chem. Commun.* **2014**, *50*, 1438−1440. (c) Zangana, K. H.; Moreno-Pineda, E.; Winpenny, R. E. P. *Dalton Trans.* **2014**, *43*, 17101−17107.
(17) lljina, E.; Korjeva, A.; Kuzmina, N.; Troyanov, S.; Dunaeva, K.; Martynenko, L. *Mater. Sci. Eng.* **1993**, 234−236.
(18) (a) Fomina, I. G.; Kiskin, M. A.; Martynov, A. G.; Aleksandrov, G. G.; Dobrokhotova, Z. V.; Gorbunova, Y. G.; Shvedenkov, Y. G.; Tsivadze, A. Y.; Novotortsev, V. M.; Eremenko, I. L. *Zh. Neorg. Khim.* **2004**, *49*, 1463−1474. (b) Zoan, T. A.; Kuzmina, N. P.; Frolovskaya, S. N.; Rykov, A. N.; Mitrofanova, N. D.; Troyanov, S. I.; Pisarevsky, A. P.; Martynenko, L. I.; Korenev, Y. M. *J. Alloys Compd.* **1995**, *225*, 396−399.
(19) Medved, T. Y.; Kabachnik, M. I. *Russ. J. Chem. B* **1954**, *3*, 255−258.
(20) (a) Sheldrick, G. M. *Acta Crystallogr.* **2008**, *A64*, 112−122. (b) Dolomanov, O. V.; Bourthis, L. J.; Gildea, R. L.; Howard, J. A. K.; Puschmann, H. *J. Appl. Crystallogr.* **2009**, *42*, 339−341. (c) Sluis, P. v. d.; Spek, A. L. *Acta Crystallogr.* **1990**, *A46*, 194−201.
(21) Bain, G. A.; Berry, J. F. *J. Chem. Educ.* **2008**, *85*, 532−536.
(22) Lopez-Dellamary, T.; Sampedro, J. A.; Carlos, G.; Fontes, M.; Ogura, T. *Transition Met. Chem.* **1978**, *3*, 342−344.
(23) Harris notation describes the binding mode as $[X{\cdot}Y_1Y_2{\cdots}Y_n]$, where X is the overall number of metals bound by the whole ligand, and each value of Y refers to the number of metal atoms attached to the different donor atoms. See Supporting Information and also: Coxall, R. A.; Harris, S. G. D.; Henderson, K.; Parsons, S.; Tasker, P. A.; Winpenny, R. E. P. *J. Chem. Soc., Dalton Trans.* **2000**, 2349−2356.
(24) (a) Yang, Y.; Walawalkar, M. G.; Pinkas, J.; Roesky, H. W.; Schmidt, H.-G. *Angew. Chem., Int. Ed.* **1998**, *37*, 96−98. (b) Walawalkar, M. G.; Roesky, H. W.; Murugavel, R. *Acc. Chem. Res.* **1999**, *32*, 117−126.
(25) (a) Jaklič, J.; Prelovsěk, P. *Phys. Rev. B* **1994**, *49*, 5065−5068. (b) Schnack, J.; Wendland, O. *Eur. Phys. J. B* **2010**, *78*, 535−541. (c) Schnack, J.; Heesing, C. *Eur. Phys. J. B* **2013**, *86*, 46.
(26) Chilton, N. F.; Anderson, R. P.; Turner, L. D.; Soncini, A.; Murray, K. S. *J. Comput. Chem.* **2013**, *34*, 1164−1175.
(27) (a) Real, J. A.; Munno, G. D.; Chiappetta, R.; Julve, M.; Lloret, F.; Journaux, Y.; Colin, J.-C.; Blondin, G. *Angew. Chem., Int. Ed. Engl.* **1994**, *33*, 1184−1186. (b) Sletten, J.; Sørensen, A.; Julve, M.; Journaux, Y. *Inorg. Chem.* **1990**, *29*, 5054−5058. (c) Charlot, M. F.; Khan, O.; Jeannin, S.; Jeannin, Y. *Inorg. Chem.* **1980**, *19*, 1410−1411.
(28) Hodgson, D. J. *Prog. Inorg. Chem.* **1975**, *19*, 173. (b) Hatfield. W. E. In *Magneto-Structural Correlations in Exchange coupled Systems*; Willett, R. D., Gatteschi, D., Kahn, O., Eds.; Reidel: Dordrecht, The Netherlands, 1984; pp 555.

DOI: 10.1021/acs.inorgchem.5b00649
Inorg. Chem. 2015, 54, 6331−6337